e-ISSN: 2550-164X

Available online at
https://jmeche.uitm.edu.my/

Journal of Mechanical Engineering 22(1) 2025, 137 – 153.

Journal of Mechanical Engineering

Quantifying Spasticity: Developing a Data-Driven Approach Through the Modified Ashworth Scale and Simulated Spasticity Model

Nurul Atiqah Othman[1], Noor Ayuni Che Zakaria[1*], Khairunnisa Johar[1], Fazah Akhtar Hanapiah[2], Natiara Mohamad Hashim[2], Cheng Yee Low[3], Jingye Yee[4]

[1]*School of Mechanical Engineering, College of Engineering, Universiti Teknologi MARA Shah Alam, Malaysia*
[2]*Faculty of Medicine, Universiti Teknologi MARA Sungai Buloh, Selangor, Malaysia*
[3]*Faculty of Mechanical and Manufacturing Engineering, Universiti Tun Hussein Onn Malaysia*
[4]*Fraunhofer Institute for Mechatronic Systems Design IEM, Paderborn, Germany*

ARTICLE INFO

Article history:
Received 6 December 2023
Revised 11 June 2024
Accepted 17 June 2024
Online first
Published 15 January 2025

Keywords:
Quantifying spasticity
Modified ashworth scale
Simulated spasticity model

DOI:
10.24191/jmeche.v22i1.4560

ABSTRACT

This study addresses the need for a quantitative assessment tool for spasticity, a common motor disorder in neurological conditions. The Simulated Spasticity Model (SSM) is developed to represent spasticity characteristics across different Modified Ashworth Scale (MAS) levels. This mathematical model captures the spasticity behaviour, offering detailed insights that qualitative descriptions cannot provide. Ethic approval was secured, and 114 data sets met the inclusion criteria. Research hypotheses, based on MAS descriptions, focused on muscle tone progression and catch positions during passive stretching. Data underwent segmentation, cleaning, and filtering, with feature extraction for crucial information. Slow passive stretch analysis revealed a quadratic characterizing range of motion (ROM) for Malaysians, exhibiting a high R^2 result of 97.36%. The fast passive stretch analysis utilized the Bi-Gaussian Peak function, creating the SSM for simplified MAS interpretation. Validation showed a significant portion of data points falling within the 0.8 to 1.0 R^2 range, confirming strong alignment with the model. Results robustly supported hypotheses, confirming the expected hierarchy of initial forces, catch positions, and graph widths. This research demonstrates that MAS can be effectively represented and understood using the SSM, bridging the qualitative-quantitative gap in spasticity assessment. In conclusion, this study transforms MAS into a data-driven tool, providing a valuable contribution to spasticity education.

[1*] Corresponding author. *E-mail address*: ayuni8098@uitm.edu.my
https://doi.org/10.24191/jmeche.v22i1.4560

INTRODUCTION

Spasticity is a complex motor disorder characterized by increased muscle tone, involuntary contractions, and movement impairments commonly observed in individuals with neurological conditions such as stroke, multiple sclerosis, and cerebral palsy (Bhimani & Anderson, 2014; Rivelis et al., 2020). The Modified Ashworth Scale (MAS) is a widely used clinical assessment tool that categorizes spasticity severity into different levels based on the resistance to passive movement (Li et al., 2017; Charalambous, 2014). However, quantifying and constructing a simulated spasticity model that accurately represents each MAS level remains a challenge. This paper presents the development of a Simulated Spasticity Model (SSM) aimed at quantifying and classifying the MAS levels of upper limb spasticity.

The objectives of this study are as follows:

(i) Quantification of MAS levels: develop a systematic approach to quantify the severity levels of MAS based on specific criteria associated with each level. This involves considering factors such as muscle tone, resistance to passive movement, and range of motion limitations.

(ii) Construction of the SSM: construct a comprehensive model that replicates the key characteristics and movement patterns associated with each MAS level. This includes factors such as muscle activation patterns, resistance profiles, and joint stiffness.

(iii) Validation and Verification: validate the SSM by comparing its output with test data. This step ensures the accuracy and reliability of the model in representing real-world spasticity levels.

Related works

Conventional upper limb spasticity assessment, and subjective evaluations using the MAS is the common practice, leading to inconsistencies in assessments. A study by Puzi et al. (2019) addressed this issue by employing a data-driven approach to analyse torque and angle signals from arm muscles. By extracting relevant features, the research aims to identify independent features for classifying spasticity levels. Notably, the findings emphasize the potential of objective data-driven approaches in enhancing spasticity assessment in rehabilitation practices. AI-driven decision-making rule for the MAS in assessing elbow flexor spasticity (Park et al., 2021). Involving 28 raters, the AI demonstrates substantial agreement (82.2%) with human assessments. Biomechanical parameters, including catch angle and stretching speed, significantly influence AI decisions, highlighting potential advancements in objective spasticity evaluations. Previous research by Adeel et al. (2023) explored the relationship between spasticity, assessed with MAS, and the active range of motion in upper limbs among chronic stroke survivors. The findings highlight the significance of AROM as a complement to subjective MAS assessments. This suggests a potential gap in the existing literature concerning the quantification and objective classification of spasticity levels. Another study by Wang et al. (2023) introduced a novel system for quantifying upper-limb spasticity severity in post-stroke patients. Although this system provides valuable insights, there is still a need for comprehensive and standardized measures that can accurately capture the nuances of spasticity. Furthermore, a study by Salau & Jain, 2019 challenges the reliability of current clinical measures, such as MAS, in accurately assessing spasticity. It underscores the need for more clinically relevant definitions and reliable measurement tools. This gap suggests the potential for developing a robust and standardized tool, such as the SSM, which could offer a more comprehensive and quantifiable representation of spasticity.

https://doi.org/10.24191/jmeche.v22i1.4560

MATERIAL AND METHODS

Research hypothesis

In this research study, MAS serves as the primary instrument for assessing the severity of spasticity. MAS plays a crucial role by providing a standardized means of quantifying muscle tone and catch behaviour in patients with spasticity (Medica et al., 2017). The research approach involves using different MAS levels as the foundation for categorizing and evaluating muscle tone and spastic catch behaviour. This approach aims to establish essential baseline parameters for the research hypothesis. The details of the hypotheses are described below.

(i) Categorizing by MAS levels: all clinical data is categorized into different MAS levels, with each level indicating a distinct degree of muscle tone and spastic catch behaviour (Bohannon & Smith, 2014) .

(ii) Measuring muscle tone: muscle tone refers to the baseline tension or resistance in a muscle when at rest (Ganguly et al., 2021). In individuals with spasticity, muscle tone can vary significantly. Therefore, the research focuses on muscle tone behaviour during passive stretch.

(iii) Assessing catch behaviour: catch behaviour refers to involuntary muscle contractions or sudden increases in resistance to passive movement, often occurring in individuals with spasticity (Rosales et al., 2011). Instances of catch behaviour are carefully observed and recorded at each MAS level.

(iv) Establish baseline parameters: by systematically measuring muscle tone and spastic catch behaviour at each MAS level, baseline parameters are established. These parameters allow for the characterization and differentiation of spasticity profiles and serve as the foundation for research hypothesis.

These parameters in ***Error! Reference source not found.*** encompass the description of the MAS. MAS levels are classified based on the progression of muscle tone and the catch's position during passive stretching (Mohamad Hashim et al., 2022; Yee et al., 2021). This description is seamlessly integrated into the SSM and serves as a reference point for each MAS level, forming the foundation for our research hypotheses. Notably, MAS 0 is characterized by "no increase in muscle tone." Since our study specifically focuses on the measurement of muscle tone and catch behaviour, data from patients with MAS 0 were excluded due to non-alignment with the criteria. Additionally, for MAS 4, characterized by rigidity in either flexion or extension of the affected part(s), insufficient data was available to support further data processing. Consequently, our analysis concentrated exclusively on MAS 1, MAS 1+, MAS 2, and MAS 3.

Table 1. Description of MAS level and hypotheses parameters

MAS	Point of reference		Hypothesis
	Muscle tone behaviour	Catch behaviour	
1	Slight increase in muscle tone	Manifested by a catch and release or by minimal resistance	**Initial force, F_S** MAS 1 < MAS 1+ < MAS 2 < MAS 3
1+	Slight increase in muscle tone	Manifested by a catch, followed by minimal resistance throughout the remainder	**Catch position θ_c** MAS 1 and MAS 1+ > HROM MAS 2 and MAS 3 < HROM
2	More marked increase in muscle tone	Through most of the ROM	**Width under the graph,** For MAS 1 and MAS 1+ $W_1 > W_2$
3	Considerable increase in muscle tone	Passive movement is difficult	For MAS 2 and MAS 3 $W_1 < W_2$

https://doi.org/10.24191/jmeche.v22i1.4560

Clinical data acquisition

This research was carried out with the approval of the Research Ethics Committee at UiTM [Ref. 600-RMI (5/1/6)] and the ethical amendment to use an updated device on 27 September 2019 (Othman et al., 2015; Yee et al., 2023). All data collection took place at UiTM Sungai Buloh Health Centre, Hospital Al Sultan Abdullah, UiTM Puncak Alam, and Daehan Rehabilitation Centre, Putrajaya. However, there were certain limitations in the selection of participants, including:

(i) Individuals must be Malaysian residents aged between 18 to 70 years.

(ii) The existence of any pathology within the central nervous system.

(iii) Patients needed to be responsive during the assessment.

The physicians who participated in this study are both experienced clinicians and educators in the field of rehabilitation medicine. To get an interrater score, data is also collected by a physiotherapist (Othman et al., 2022) Before the data collection process, the patients and their caregivers received a comprehensive explanation of the entire procedure. Prior to commencing the data collection, informed consent and the respective signatures from the patients or their caregivers were obtained.

The assessment comprised two phases: slow and fast passive stretches, each repeated three times by a different rater. Slow passive stretches aimed to determine the range of motion (ROM) of the examined joint. And fast passive stretches focused on identifying the catch and muscle tone behaviour. These angles and force measurements were recorded. During the clinical assessment, patients were positioned lying down with their arms alongside their bodies. As depicted in Fig. 1, the assessment is done from sROM (full flexion position) to eROM (full extension position).

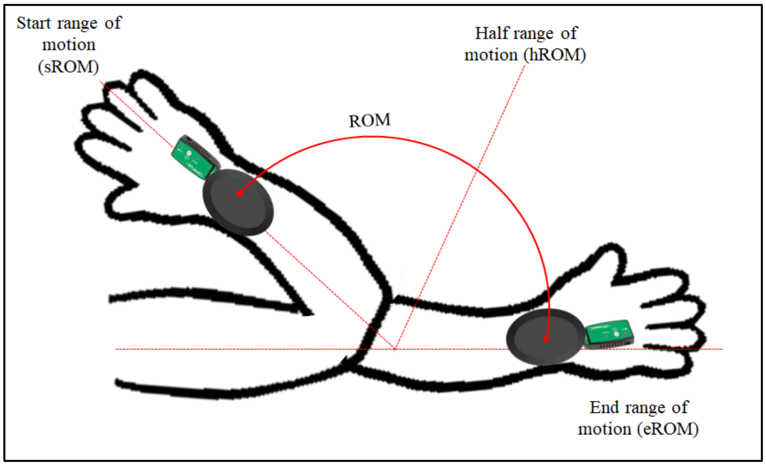

Fig. 1. Illustration of flexion-extension stretch during clinical assessment.

In Fig. 2, the wireless data acquisition system utilized during the clinical assessment was provided by Biometrics Ltd. This system included a twin-axis electrogoniometer for angle measurement and a MyoMeter to quantify force and resistance during the clinical assessment. All these components were connected via wireless to DataLite PC software version 10.28, enabling the recording of data during the assessment. The wireless sensors collected signals and transmitted them to a data acquisition terminal, which was a local computer, using a dongle wireless transceiver. This computer was equipped with the DataLITE data acquisition software (ver. 10.28) from Biometrics Ltd. (Yee et al., 2023). All the signals were then forwarded to the DataLITE software for further analysis.

https://doi.org/10.24191/jmeche.v22i1.4560

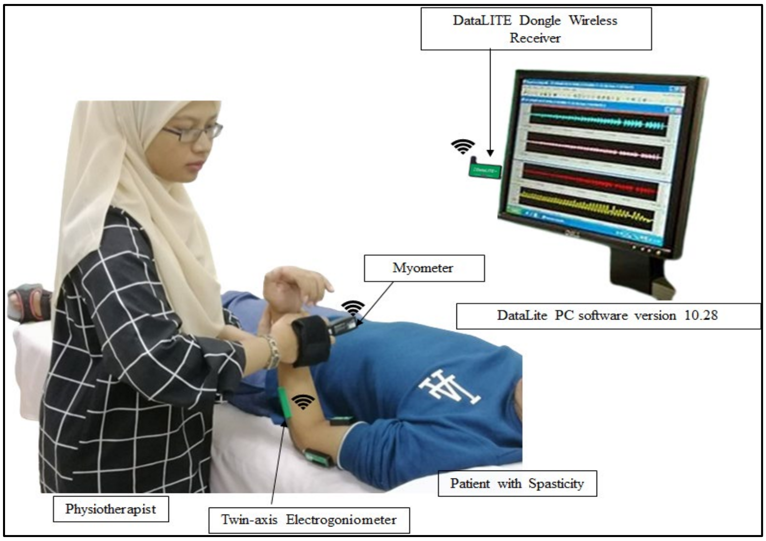

Fig. 2. The placement of Twin-axis Goniometer and Myometer during clinical assessment.

Data pool

A total of 76 patients with spasticity were recruited for the study, and the mean age was 49.27 years with a standard deviation of 18.81. Clinical data were collected by different raters (expert physicians and physiotherapists), resulting in a total of 114 datasets. The distribution of MAS ratings is detailed in Table 2, The primary cause of spasticity was stroke, followed by cerebral palsy, meningitis, traumatic brain injury, spinal cord injury, Hypoxic-Ischemic Encephalopathy, and Parkinson's disease. Three (3) datasets were excluded from the analysis due to the non-responsiveness of patients during clinical assessments.

Table 2. Distribution of MAS level from the clinical assessment

MAS level	0	1	1+	2	3	4	Total
Trials	28	43	25	10	6	2	114

Out of the 114 datasets, several criteria are excluded. These exclusion criteria were as follows:

(i) Individuals with elbow joints or forearm pathology not related to neurological causes.

(ii) Participants with elbow joint contractures caused by bone pathology.

(iii) Patients are diagnosed with cerebral palsy (CP). This decision was informed by the observation that individuals with CP often demonstrate active stretching during the assessment, which makes it challenging to accurately define the force at the biceps.

(iv) Participants who had undergone botulinum toxin treatment.

(v) Data associated with MAS 0 and MAS 4, as previously detailed in the research hypothesis (Table 1).

Every dataset is comprised of three sets of slow stretch data and three sets of fast stretch data, resulting in a total of 342 data for fast stretches and 342 for slow stretches. Following the exclusion criteria above, 184 data are devoted to slow stretches and 184 data to fast stretches. The distribution across different MAS levels is visually presented in Table 3.

https://doi.org/10.24191/jmeche.v22i1.4560

Table 3. Distribution of MAS level after applying the exclusion criteria

MAS level	1	1+	2	3	Total
Fast stretch	87	66	27	6	186
Slow stretch	87	66	27	6	186

Data pre-processing

The pre-processing procedure as in Fig. 3 commences with data segmentation, followed by data cleaning and filtering, and finally, feature extraction, resulting in the generation of the desired features.

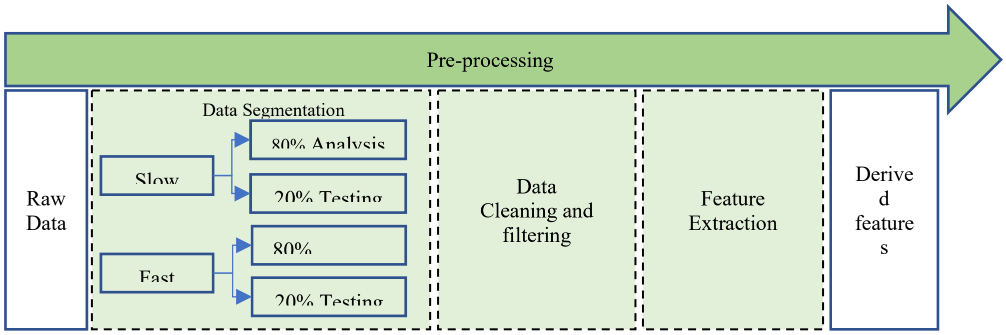

Fig. 3. Pre-processing procedure to convert raw data into desired features.

Data segmentation

During the data segmentation process, the data is selected and classified based on the MAS level, aligning with the rater classification. The data is divided into two distinct groups: i) slow stretch aimed at assessing the range of motion (ROM), while ii) fast stretch used to evaluate Initial force, catch position, and the area under the graph both before and after the catch has occurred. All the data is subdivided into two segments. 80% of the data is earmarked for analysis, while the remaining 20% is set aside for testing and evaluation purposes.

Collected clinical data is obtained from DataLite PC software version 10.28. Data recorded from myometer is in Newtons (N), and the twin-axis goniometer provides data in degrees (°) for two axes (x-axis and y-axis) (Yee et al., 2023). To compute the elbow angle from the goniometer data, the angular measurements are treated as Cartesian coordinates. The resultant angle is calculated using the Pythagorean theorem:

$$\text{Elbow angle}, \theta \ (°) = \sqrt{(\theta_x^{\,2} + \theta_y^{\,2})} \tag{1}$$

This method is derived from the elbow angle by combining the contributions from both axes, facilitating further analysis.

Data cleaning and filtering

Upon consolidating all the data into each respective group, the next step in the process is data cleansing. This step is crucial because the data, being in the waveform, exhibits uneven sampling, and since all the sensors are wireless, the signal tends to be noisy. To extract the essential information required for signal evaluation, the locally weighted scatterplot smoothing (LOWESS) method is employed. LOWESS is a non-

https://doi.org/10.24191/jmeche.v22i1.4560

parametric regression technique (Fotiadis et al., 2016; Dias & Ronaldo, 2008). which involves an analytical approach aimed at generating a set of points along a curve. This process serves the purpose of eliminating noise from the raw clinical data. Subsequently, each graph is examined to discern the trends of each MAS level.

A sample of raw clinical data is depicted in Fig. 4, sourced from patient 25, a male individual with post-ischemic stroke. The irregular distribution of data points emphasizes the superiority of the LOWESS approach in assessing the necessary and significant spasticity behaviour.

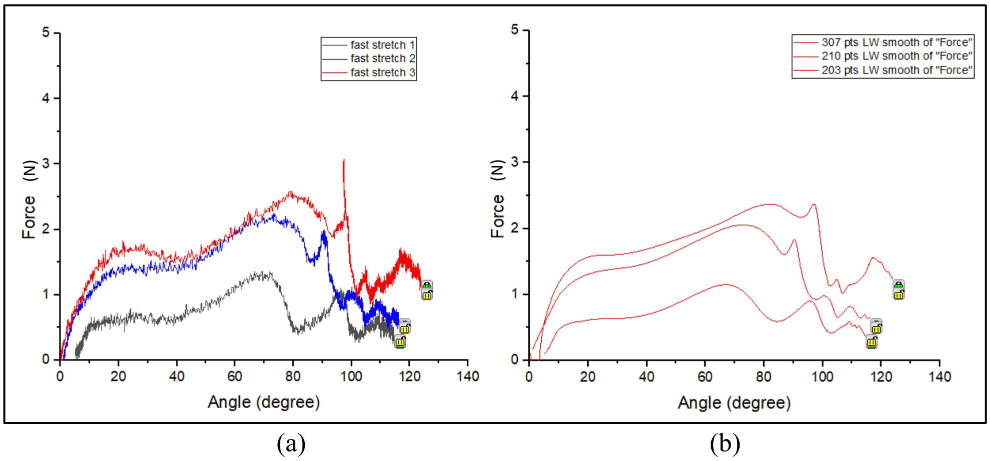

Fig. 4. Sample (a) before and (b) after applying the LOWESS method of fast passive stretch.

Feature extraction

This process involves systematically identifying and distilling crucial information from clinical data, with a particular focus on shape features (Salau & Jain, 2019). These shape features encompass initial force, catch position, and the width under the graph before and after the catch, all of which play a vital role in characterizing spasticity behaviour. They offer a comprehensive view of muscle tone and resistance to passive movement which only occurs at fast stretches. That information contributes to understanding and quantifying spasticity.

(i) Initial force (F_S): This feature represents the force exerted at the onset of passive stretch, helping gauge initial force during movement, and providing insights into muscle tone.

(ii) Catch position (θ_C): Catch position marks the point at which a rapid increase in muscle activation results in an abrupt stop or heightened resistance during a fast passive stretch. This parameter is vital for recognizing the catch phenomenon associated with spasticity.

(iii) Width under the graph (W_1 and W_2): The width under the graph before and after the catch is an indicator of cumulative muscle activation and resistance exhibited by patients. It provides an integrated perspective on spasticity's severity and characteristics, making it essential for differentiating between MAS levels.

(iv) Height (H): Indicate the height of force captured during catch at θ_C from F_S.

To make sense of the data, a nonlinear curve fitting feature is used to consider every significant parameter. A Bi-gaussian function is employed to obtain peak modelling as in Fig. 5. The result is represented as the SSM, consisting of five parameters: initial force, catch position, height, and the width

https://doi.org/10.24191/jmeche.v22i1.4560

under the graph before and after the catch. This alignment makes the Bi-Gaussian function an ideal morphological tracking algorithm for accurately capturing the curve of spasticity.

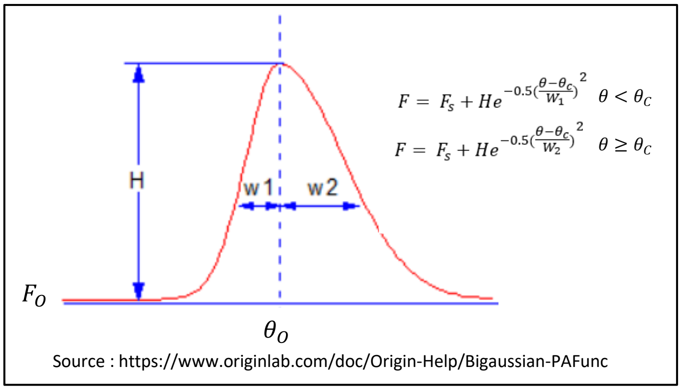

Fig. 5. Sample curve and parameters involved.

The feature extraction process aligns with several overarching research objectives:

(i) Pattern recognition: By extracting shape features, the research aims to recognize distinct patterns in spasticity behaviour across different MAS levels. These patterns serve as the foundation for a quantitative model of spasticity.

(ii) Visualization: The extracted features are visualized to enhance the comprehension of spasticity data's shape and structure. This aids in the interpretation and communication of findings.

(iii) Improved model performance: The feature-extracted data optimizes the efficiency and effectiveness of data mining techniques, enhancing the performance of the simulated spasticity model.

(iv) Interpretability: The features selected for extraction are chosen for their relevance and interpretability, ensuring that the model's results are meaningful and actionable in a clinical context.

To obtain the range of motion, slow stretch data analysis is also essential. This analysis provides the range of motion and identifies where the initial force and catch position occur. The positions of these parameters are derived from slow stretch data, which is crucial for understanding the complete spasticity profile.

RESULTS AND DISCUSSION

Classification

This research section explained the quantification and identification of distinct patterns associated with spasticity, with a specific focus on MAS 1, MAS 1+, MAS 2, and MAS 3. The classification procedure encompasses two primary phases. As shown in **Error! Reference source not found.**, the first phase involves an analysis of slow stretch data, extracting essential parameters like Passive Range of Motion (pROM), start Range of Motion (sROM), half Range of Motion (hROM), and end Range of Motion

https://doi.org/10.24191/jmeche.v22i1.4560

(eROM). Subsequently, the research shifts its attention towards identifying the core characteristics embedded within fast stretch data, aligning these attributes with MAS 1, MAS 1+, MAS 2, and MAS 3. This dynamic approach aims to provide a comprehensive comprehension of the intricate spasticity patterns as a strong foundation for effective classification and model development.

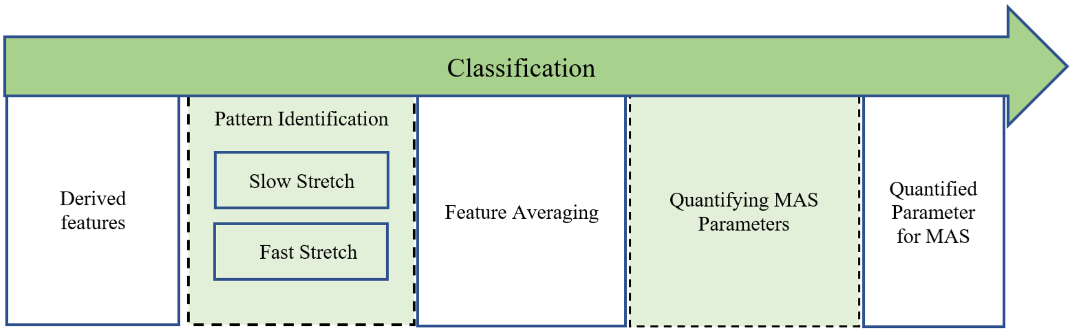

Fig. 6. Classification procedure to obtain parameters and patterns for ROM and MAS level.

A core component of pattern identification is feature averaging, a technique of significant value. This method entails calculating the average of multiple graphs to derive a representative parameter. The use of the averaging method is important because it helps mitigate the impact of outliers and variability inherent in individual measurements. By averaging multiple datasets, the resultant average graph smooths out anomalies and highlights the most consistent patterns, leading to more reliable findings. This is crucial for characterizing spasticity patterns and ensuring the robustness of the classification model.

The analysis was conducted using OriginPro 2021, employing the feature averaging technique. The method selected for feature averaging was 'average,' with specific settings configured to optimize the process. The 'Average X value' was set as ‘Full X range’ with 1000 points, and linear interpolation was applied. This approach ensures a comprehensive and accurate representation of the patterns, making it a pivotal element in the classification process.

After the classification phase, the next step involves regression analysis, with a particular focus on the simulated curve feature. The data obtained from feature averaging is refined by using a nonlinear curve fitting technique that considers all essential spasticity parameters. Then, the feature averaging profile is simulated by using suitable nonlinear curve fitting to construct the simulated model.

To enhance the representational accuracy and power of the simulated model, an evaluation process is employed. This process involves testing the simulated model used for both slow and fast stretch analysis with a 20% test dataset that was separated during the initial data segmentation process. The evaluation results are quantified using R^2 values, which serve as indicators of the similarity between the simulated model and the test data.

Slow passive stretch analysis

This section primarily focuses on determining parameters for: pROM, sROM, hROM, and eROM, derived from slow stretch data analysis. Descriptive statistics are applied to this dataset to establish a baseline understanding of the central tendencies and variability within the slow stretch dataset.

Subsequently, as shown in Fig. 7, the analysis delves deeper into pattern identification through the feature averaging process. This phase allows us to uncover underlying patterns within the dataset. Once these patterns are identified, nonlinear curve fitting is employed. Specifically, a quadratic polynomial function is used for curve fitting. The decision to use a quadratic function to model human arm movement

https://doi.org/10.24191/jmeche.v22i1.4560

is because the arm moves in one primary direction (flexion-extension movement). The result, with an R^2 value of 0.9966, indicates an excellent fit between the curve and the data. An R^2 value approaching 1 reflects the model's strong capacity to explain the data's variability. Equation (2) characterizes a fitted curve, with a, b, and c representing coefficients that define the curve's shape. The result in Table 4 shows the mean and standard deviation (SD) of sROM, eROM, pROM, and hROM.

$$\theta(t) = at^2 + bt + c \tag{2}$$

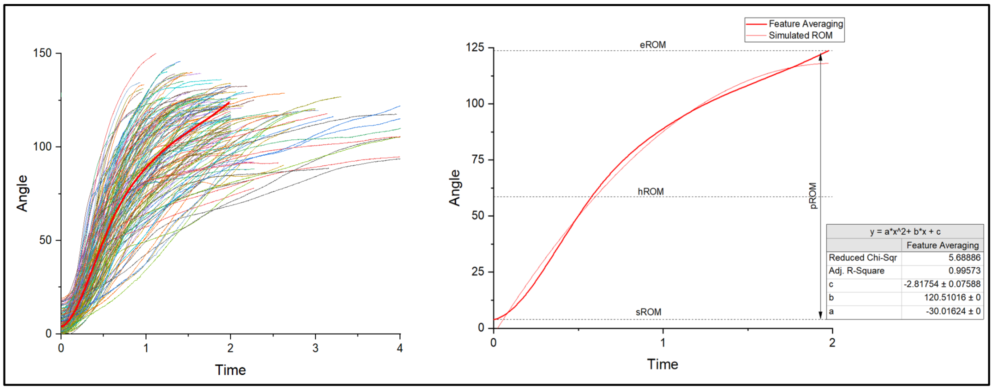

(a) (b)

Fig. 7. (a) Feature averaging and (b) nonlinear curve fitting analysis on slow stretch data.

Table 4. Mean and standard deviation for sROM, eROM, pROM, and hROM

	sROM	eROM	pROM	hROM
Mean (degree)	3.86	123.72	120.19	58.58
Standard deviation	3.52	8.57	8.28	5.08

In the context of this research, the variables in the polynomial equation are defined as,

(i) θ: represents the dependent measure, specifically, the pROM. It indicates the extent of joint movement in the spastic arm.

(ii) t: an independent variable in our research is time, which serves as the observed parameter influencing the dependent variable (θ).

The coefficients of a, b, and c are components of the polynomial equation, shaping the resulting curve to fit the data.

(i) a, the coefficient of the quadratic term captures how time (t) has a squared or quadratic effect on pROM (θ). This term is responsible for introducing curvature to the curve, reflecting the complex relationship between time and pROM in the spastic arm.

(ii) b, as the coefficient of the linear term represents how changes in time (t) linearly affect pROM (θ). This component indicates the influence of time on pROM in a straightforward, linear manner, and

(iii) c, the interception signifies the value of pROM when time (t) is zero. Essentially, it provides the y-value where the curve meets the y-axis, offering a reference point for pROM.

https://doi.org/10.24191/jmeche.v22i1.4560

The analysis demonstrates thoroughness, with a high R^2 value indicating an effective curve fit to the data. However, it's crucial to assess whether the model aligns with theoretical expectations and clinical insights and to consider the practical significance. Testing the equation on the test dataset provides a valuable evaluation process. From the results, the R^2 result of 97.36%, mostly falling within the 0.9 to 1 range, shows the formula's excellent fit to the initial data. The remaining 2.63% of data, with R^2 values between 0.8 and 0.9, still represent a strong fit, possibly due to unaccounted factors or data noise.

Fast passive stretch analysis

In this section, our focus centers on a comprehensive analysis of the MAS, with specific emphasis on MAS levels 1, 1+, 2, and 3. Our primary objective is to uncover and decipher the intricate muscle tone profile exhibited within these spasticity levels. After obtaining the profiles of MAS 1, 1+, 2, and 3 through a feature averaging procedure, a thorough inspection is pursued to verify that each profile adheres to the characteristics outlined by the MAS descriptions.

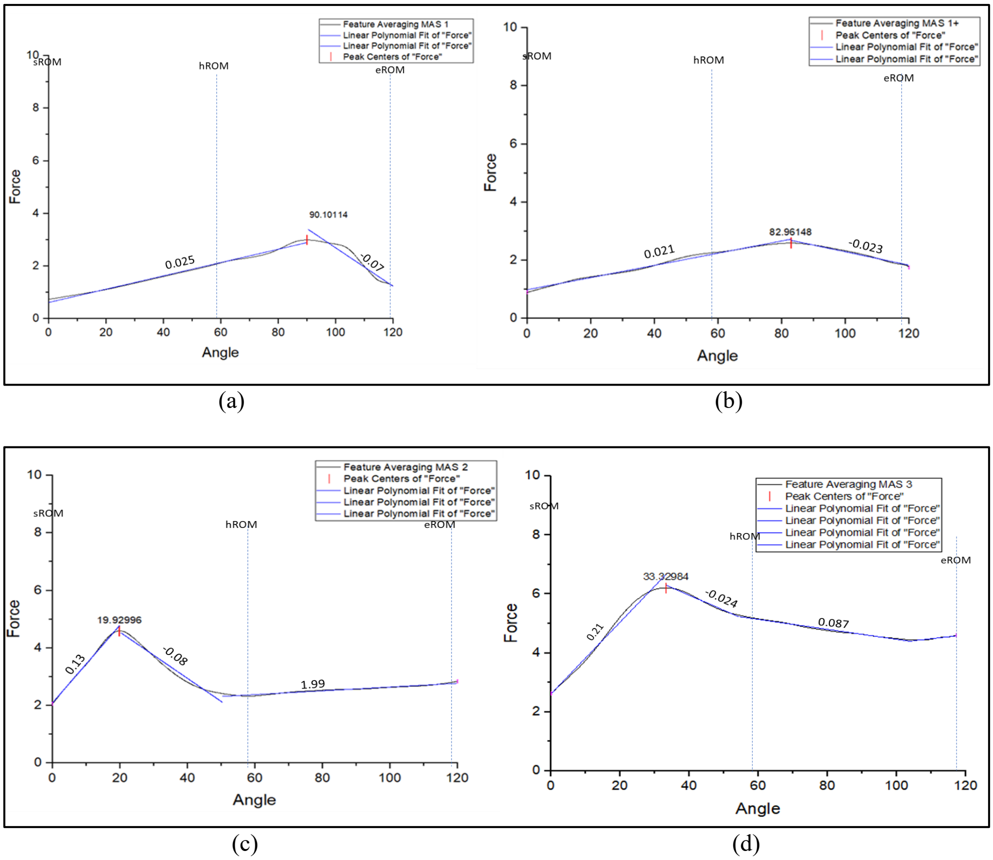

Fig. 8. Feature averaging and linear fit (a) MAS 1, (b) MAS 1+, (c) MAS 2 and (d) MAS 3.

The analysis of the force vs. angle graph for MAS 1 provides valuable insights into the specific characteristics of this level of spasticity. Fig. 8(a) shows that the observed slope for MAS 1 is 0.025 with R^2 0.992 from 0.14° to 90.10° reflects a gradual increase in force with changing angles, indicating a slight augmentation in muscle tone as the range of motion progresses. This aligns with the description of MAS 1, where there is indeed a mild increase in muscle tone, yet it is not notably intense or rigid. Catch is

https://doi.org/10.24191/jmeche.v22i1.4560

characterized by a brief resistance and is followed by a subsequent reduction in muscle tone, leading to minimal resistance towards the end of the range of motion. It is shown at the slope after the catch, which is -0.07 with R^2 0.94, indicating a further reduction in muscle tone beyond the catch point. The negative force value signifies a decline in force compared to the previous angle, reinforcing the idea of release in muscle tone.

For MAS 1+, the description of a "slight increase in muscle tone" is reflected in the data. Referring to Fig. 8(b), the catch, observed at 82.96° with a force of 2.59 N, corresponds to a point where muscle tone exhibits an abrupt but relatively mild increase, as indicated by a sudden elevation in force. This finding aligns with the description of MAS 1+, where a catch has occurred after hROM and higher muscle tone is identified. The slope of 0.02 and R^2 0.991 from the start of the passive stretch indicates a gradual force increase over the range of motion. However, after the catch, the slope changes to -0.023 with R^2 0.98, reflecting a reduction in muscle tone, consistent with the description of "minimal resistance" throughout less than half of the range of motion. This subtle reduction in muscle tone is consistent with the observation of a catch followed by minimal resistance, as described in MAS 1+.

In the analysis of MAS 2, the description of a "more marked increase in muscle tone through most of the ROM" is clearly reflected in the data in Fig. 8(c). The initial force of 2.06 N and the subsequent increase to 4.69 N during the catch angle at 19.92° align with this description, indicating a substantial and noticeable increase in muscle tone. The relatively steep slope of 0.13 with R^2 0.997 signifies a significant rise in force as the angle changes, supporting the concept of increased muscle tone in MAS 2. Post-catch, the graph transitions to a negative slope of -0.08, accompanied by an R^2 value of 0.97. This decline signifies a reduction in muscle tone, reflecting the MAS 2 characteristic where specific muscle parts become more easily movable. Subsequently, an increasing pattern emerges with a slope of 1.99 and an R^2 value of 0.96, signifying slight resistance in muscle tone towards the end of the range of motion.

The MAS 3 spasticity profile aligns with the description of a marked increase in muscle tone, with the affected part still moveable. Commencing with the pattern of MAS 3 in Fig. 8(d), the high initial force is at 2.63 N, the graph demonstrates elevated muscle tone at sROM. The steep slope of 0.21 (R^2 0.987) leading from 0° to 33.32°, accompanied by a force increase from 2.63 N to 6.21 N, signifies a rapid escalation in force. It illustrates a sudden increase in muscle tone at sROM. Following the catch, the force experiences a slight decrease to 4.49 N, depicted by a slope (-0.024, R^2 0.93) and followed by an increasing slope (0.087, R^2 0.75). Referring to the trend in both slopes, it is indicating a sustained higher resistance than MAS 2 throughout the ROM.

The research proceeds to simulate the MAS profile through the Simulate Curve feature by OriginPro 2021. This simulation is built upon the foundation of the Bi-Gaussian Peak function, a mathematical model to replicate the spasticity profile. The choice of this function stems from its exceptional capacity to precisely capture the essential parameters, including initial force, catch position, and the width under the graph before and after the catch, all integral to the understanding of spasticity dynamics. Through the application of the Bi-Gaussian Peak function (Marcotte & David, 1985; Yu & Peng, 2010), the research generates an equation that captures the dynamics of spasticity, providing a quantitative representation.

$$F = F_S + He^{-0.5(\frac{\theta-\theta_C}{W_1})^2} \quad \theta < \theta_C \tag{3}$$

$$F = F_S + He^{-0.5(\frac{\theta-\theta_C}{W_2})^2} \quad \theta \geq \theta_C$$

where F_s is the initial force, θ_c is the angle at catch, W_1 is the width before catch, W_2 is the width after catch, and H is height.

https://doi.org/10.24191/jmeche.v22i1.4560

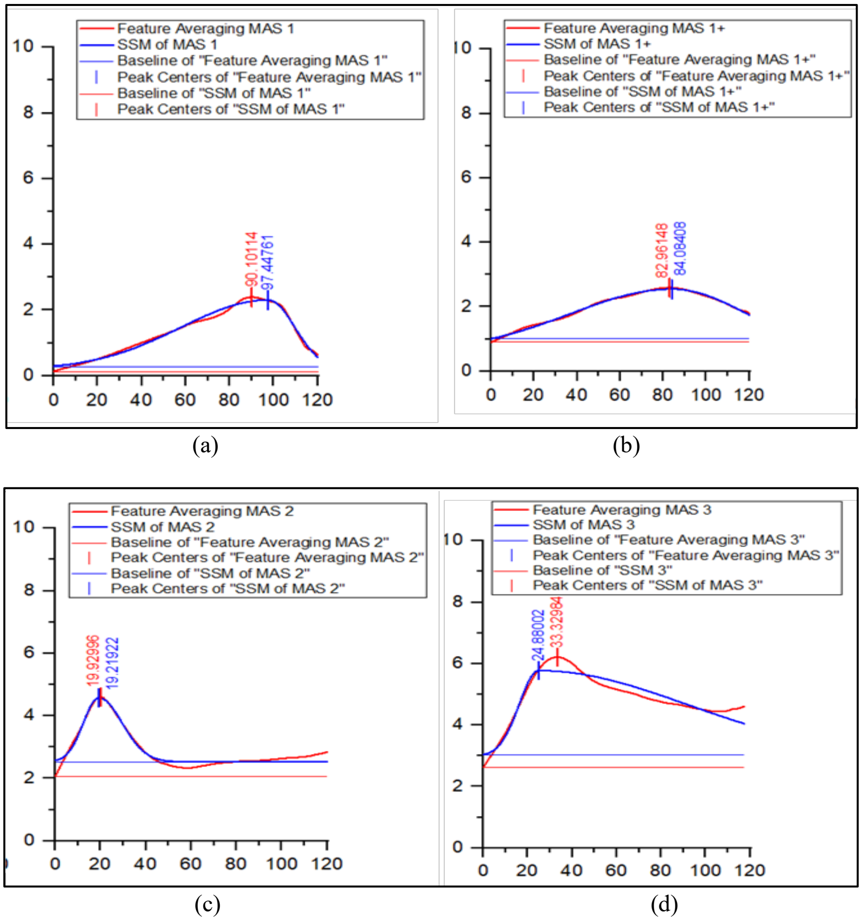

Fig. 9. Simulated Spasticity Model (SSM) fitted with Feature Averaging, (a) MAS 1, (b) MAS 1+, (c) MAS 2, and (d) MAS 3.

Table 5. R^2 value and parameters of Bi-Gaussian peak function

	MAS 1		**MAS 1+**		**MAS 2**		**MAS 3**	
R^2	0.99		0.99		0.96		0.92	
Parameters								
	Value	SE	Value	SE	Value	SE	Value	SE
Initial force, $\boldsymbol{F_S}$	0.19	0.01	0.60	0.01	2.53	0.00	2.99	0.05
Angle at catch, $\boldsymbol{\theta_c}$	97.54	0.13	84.12	0.14	19.19	0.11	24.85	0.35
Height, $\boldsymbol{H}$	2.12	0.01	1.95	0.01	2.05	0.01	2.78	0.05
Width before catch, $\boldsymbol{W_1}$	39.70	0.30	47.33	0.35	6.85	0.10	8.73	0.40
Width after catch, $\boldsymbol{W_2}$	12.11	0.13	34.90	0.20	10.31	0.11	66.52	0.96

https://doi.org/10.24191/jmeche.v22i1.4560

These simulated curves are created using the Bi-Gaussian Peak function as in Equation (3), each representing a distinct MAS level as shown in Fig. 9, and the specific parameters are detailed in

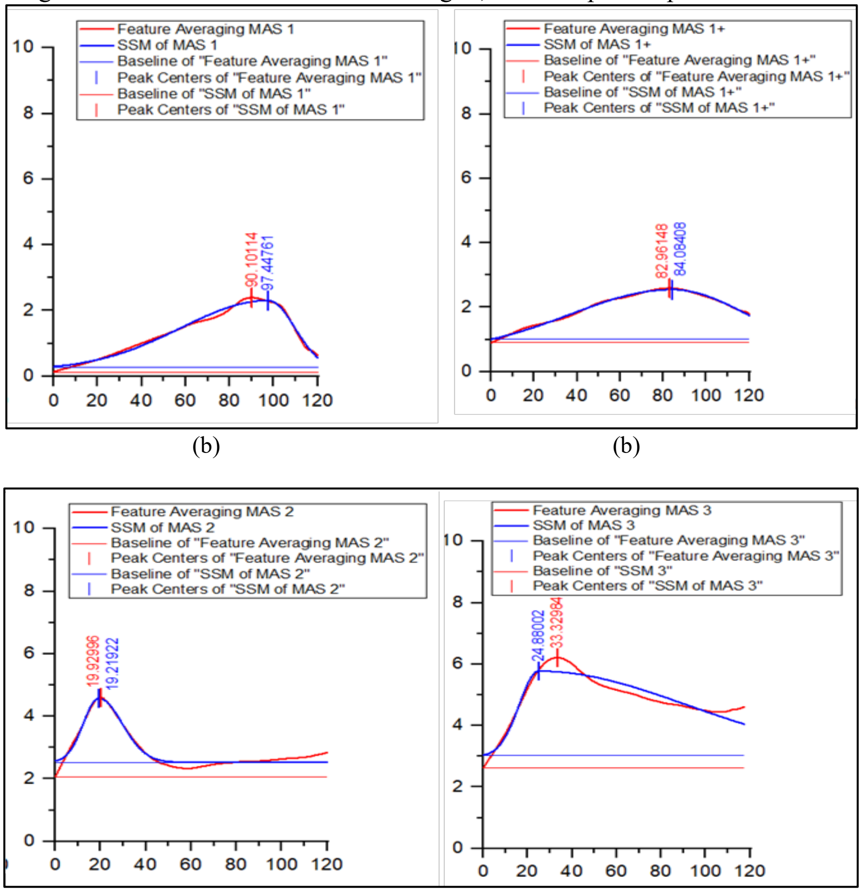

(b) (b)

(c) (d)

Fig. 9. Simulated Spasticity Model (SSM) fitted with Feature Averaging, (a) MAS 1, (b) MAS 1+, (c) MAS 2, and (d) MAS 3.

Table 5. When comparing the results of ULSTraD's R^2 values for MAS 1, 1+, 2, and 3 (0.99, 0.99, 0.96, and 0.92, respectively) with other research in Table 6, ULSTraD shows a remarkable level of accuracy and consistency. For example, Zhang et al. (2019) reported an R^2 value of 0.93 using linear regression, which is similar to ULSTraD's performance. Other studies, like Yee et al. (2023) and J. Park et al. (2021), reported accuracy and correlation coefficients that indicate strong but slightly lower levels of correlation (91% accuracy and 0.825, respectively). This comparison highlights ULSTraD's superior ability to simulate spasticity, as it achieves a higher degree of fidelity in its spasticity representation compared to these previous models.

Table 6. Result from another related research

Study	Model type	R^2 value
Yee et al., 2023	Not specified	Accuracy and F1: 91%
J. Park et al., 2021	AI model	Correlation coefficient: 0.825
Zhang et al., 2019	Linear regression	0.93

https://doi.org/10.24191/jmeche.v22i1.4560

Puzi et al., 2019	SVM, LDA, KNN	84%, 80%, 76%
Pandyan et al., 2001	Non-linear curve	0.844

The evaluation process effectively validates the SSM generated through the Simulate Curve feature and the Bi-Gaussian Peak function, particularly for MAS 1, MAS 1+, MAS 2, and MAS 3. Hence, Fig 10 visually represents the feature averaging and the SSM for each MAS level.

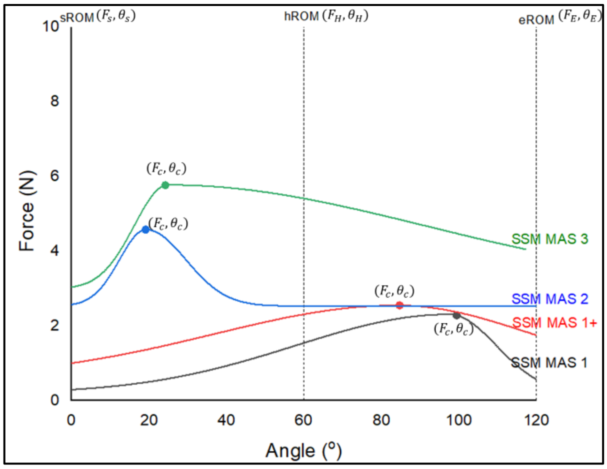

Fig. 10 Simulated Spasticity Model (SSM)

CONCLUSION

The primary objective of this research is to transition the Modified Ashworth Scale (MAS) from a qualitative assessment tool for spasticity to a quantitative and data-driven assessment. Currently, in rehabilitation centres, hospitals, and medical schools, MAS is widely employed to assess spasticity, but its application is primarily qualitative, lacking numerical values and specific parameters. This study aims to bridge this gap by introducing a quantitative framework to evaluate and understand spasticity. In the context of slow stretch analysis, quadratic function withstands out as a valuable tool for interpreting the range of motion (ROM) in the human arm. Given that the data was collected in Malaysia, the results provide specific insights into the ROM characteristics of the Malaysian demographic. The findings also serve as a reference point, offering limits for the start range of motion (sROM), half range of motion (hROM), end range of motion (eROM), and passive range of motion (pROM). These quantifiable parameters can significantly enhance the understanding of spasticity, especially in the context of human arm movement. Additionally, the results provide valuable data on the positioning of the "catch" phenomenon during fast extension, the critical aspect of spasticity assessment. In fast stretch analysis, the datasets gathered from clinical assessments have proven to be robust and suitable for the analysis. Table 7 shows analysis results affirm the satisfaction of the hypotheses.

Table 7. Hypothesis and analysis result

Hypothesis	Result
Initial force, F_S MAS 1 < MAS 1+ < MAS 2 < MAS 3	**Initial force, F_S** MAS 1 = 0.19 N, MAS 1+ = 0.60 N, MAS 2 = 2.53 N, MAS 3 = 2.99 N MAS 1 < MAS 1+ < MAS 2 < MAS 3

https://doi.org/10.24191/jmeche.v22i1.4560

Catch position θ_c MAS 1 and MAS 1+ > hROM MAS 2 and MAS 3 < hROM	**Catch position θ_c** hROM = 58.58° MAS 1 = 97.54°, MAS 1+ = 84.12° MAS 1 and MAS 1+ > hROM MAS 2 = 19.19°, MAS 3 = 24.85° MAS 2 and MAS 3 < hROM
Width under the graph, For MAS 1 and MAS 1+ $W_1 > W_2$ For MAS 2 and MAS 3 $W_1 < W_2$	**Width under the graph,** MAS 1 ; W_1 = 39.70, W_2 = 12.11 MAS 1+ ; W_1 = 47.33, W_2 = 34.90 MAS 1 and MAS 1+ : W1 > W2 MAS 2 ; W_1 = 6.85, W_2 = 10.31 MAS 3 ; W_1 = 8.73, W_2 = 66.52 For MAS 2 and MAS 3: W1 < W2

The research strongly suggests that spasticity can be effectively represented and understood using the Bi-Gaussian Peak function. The Simulated Spasticity Model (SSM) emerges as an essential tool, making the interpretation of spasticity more comprehensible. It simplifies the understanding of all the parameters outlined in the MAS descriptions, allowing for easy interpretation from the graphical representations.

In conclusion, this research successfully bridges the qualitative-quantitative divide in spasticity assessment by transforming the MAS into a data-driven tool. The SSM can serve as a baseline for recreating spasticity behaviour using a high-fidelity upper limb spasticity simulator. The goal is to improve the teaching and learning process for clinical trainees. By providing a detailed and data-driven representation of spasticity, the SSM enhances the educational tools available for understanding and managing spasticity in clinical settings. Recommendations include expanding datasets for further exploration of MAS levels and ensuring a comprehensive understanding of spasticity. This research pioneers a transformative approach, enhancing spasticity assessment for both clinical and educational purposes.

AUTHORS' CONTRIBUTIONS

The authors confirm equal contributions in each part of this work. All authors reviewed and approved the final version of this work.

FUNDING

The authors would like to acknowledge the support of the College of Engineering, Universiti Teknologi MARA (UiTM), Journal Support Fund UiTM, and Institute of Graduate Studies (IPSiS) UiTM, for providing the facilities and financial support for this research.

CONFLICT OF INTERESTS STATEMENT

The authors agree that this research was conducted in the absence of any self-benefits, commercial, or financial conflicts and declare the absence of conflicting interests with the funders.

REFERENCE

Adeel, M., Peng, C. W., Lee, I. J., & Lin, B. S. (2023). Prediction of spasticity through upper limb active range of motion in stroke survivors: A generalized estimating equation model. Bioengineering, 10(11),

https://doi.org/10.24191/jmeche.v22i1.4560

1273.

Bhimani, R., & Anderson, L. (2014). Clinical understanding of spasticity: Implications for practice. Rehabilitation Research and Practice, 2014(8), 279175. https://doi.org/10.1155/2014/279175

Bohannon, R. W., & Smith, M. B. (2014). Interrater reliability of a modified ashworth scale of muscle spasticity. Classic Papers in Orthopaedics, 415–417. https://doi.org/10.1007/978-1-4471-5451-8_105

Dias, Ronaldo. (2008). Nonparametric Regression: Lowess/Loess (pp. 1–4). University of Campinas.

Fotiadis, D. A., Astaras, A., Kalfas, A., & Bamidis, P. D. (2016). A novel signal processing method based on the frequency modality for intra-body medical instrument tracking. International Conference on Modern Circuits and Systems Technologies, MOCAST (pp. 16–19). IEEE Publishing. https://doi.org/10.1109/MOCAST.2016.7495123

Ganguly, J., Kulshreshtha, D., Almotiri, M., & Jog, M. (2021). Muscle tone physiology and abnormalities. Toxins, 13(4), 282. https://doi.org/10.3390/toxins13040282

Li, X., Shin, H., Li, S., & Zhou, P. (2017). Assessing muscle spasticity with Myotonometric and passive stretch measurements: Validity of the Myotonometer. Scientific Reports, 7, 44022. https://doi.org/10.1038/srep44022

Marcotte, D., & David, M. (1985). The Bi-Gaussian approach: A simple method for recovery estimation. Journal of the International Association for Mathematical Geology, 17(6), 625–644. https://doi.org/10.1007/BF01030857

Meseguer-Henarejos A. B., Sánchez-Meca J., López-Pina J. A., & Carles-Hernández R. (2018). Inter- and intra-rater reliability of the Modified Ashworth Scale: A systematic review and meta-analysis. European Journal of Physical and Rehabilitation Medicine, 54(4), 576-590. https://doi.org/10.23736/S1973-9087.17.04796-7

Othman, N. A., Che Zakaria, N. A., Hanapiah, F. A., Mohamad Hashim, N., Johar, K., Low, C. Y., & Yee, J. (2022). Quantifying the performance of wireless data acquisition system to assess upper limb spasticity. International Symposium in Robotics and Manufacturing Automation, ROMA (pp. 1-4). IEEE Publishing.

Othman, N. A., Che Zakaria, N. A., Yee Low, C., Hanapiah, F. A., Komeda, T., & Inoue, K. (2015). Towards a clinically compliant upper limb part-task trainer in simulated learning program. Jurnal Teknologi, 76(4), 71–76.

Pandyan, A, Malhotra, S., Cousins, E., Ward, A., Day, C., Jones, P.,& Roffe, C. (2008). An investigation into the agreement between clinical, biomechanical and neurophysiological measures of spasticity. Clinical rehabilitation, 22(12), 1105–1115. https://doi.org/10.1177/0269215508095089.

Park, J. H., Kim, Y., Lee, K. J., Yoon, Y. S., Kang, S. H., Kim, H., & Park, H. S. (2019). Artificial Neural Network learns clinical assessment of spasticity in modified Ashworth scale. Archives of Physical Medicine and Rehabilitation, 100(10), 1907–1915. https://doi.org/10.1016/j.apmr.2019.03.016

Puzi, A. A., Sidek, S. N., Yusof, H. M., & Khairudin, I. (2019). Objective analysis of muscle spasticity level in rehabilitation assessment. International Journal of Integrated Engineering, 11(3), 223-231. https://doi.org/10.30880/ijie.2019.11.03.023

Rivelis, Y., Zafar, N., & Morice, K. (2023). Spasticity. Treatment/Management (pp. 1–7). StatPearls Publishing.

https://doi.org/10.24191/jmeche.v22i1.4560

Rosales, R. L., Kanovsky, P., & Fernandez, H. H. (2011). What's the "catch" in upper-limb post-stroke spasticity: expanding the role of botulinum toxin applications. Parkinsonism & Related Disorders, 17(1), 3-10. https://doi.org/10.1016/j.parkreldis.2011.06.019

Salau, A. O., & Jain, S. (2019). Feature extraction: A survey of the types, techniques, applications. International Conference on Signal Processing and Communication, ICSC, (pp. 158–164). IEEE Publisher.

Wang, C., Peng, L., Hou, Z. G., Zhang, P., & Fang, P. (2023). An easy-to-use assessment system for spasticity severity quantification in post-stroke rehabilitation. IEEE Transactions on Cognitive and Developmental Systems, 16(3), 828-839. https://doi.org/10.1109/TCDS.2023.3304352

Yee, J., Low, C. Y., Mohamad Hashim, N., Che Zakaria, N. A., Johar, K., Othman, N. A., Chieng, H. H., & Hanapiah, F. A. (2023). Clinical spasticity assessment assisted by machine learning methods and rule-based decision. Diagnostics, 13(4), 739. https://doi.org/10.3390/diagnostics13040739

Yu, T., & Peng, H. (2010). Quantification and deconvolution of asymmetric LC-MS peaks using the bi-Gaussian mixture model and statistical model selection. BMC Bioinformatics, 11(1), 559. https://doi.org/10.1186/1471-2105-11-559

https://doi.org/10.24191/jmeche.v22i1.4560